Bacillus thuringiensis Cry1Ac toxin interaction with *Manduca sexta* aminopeptidase N in a model membrane environment

Matthew A. COOPER*, Joe CARROLL†, Emma R. TRAVIS†[1], Dudley H. WILLIAMS* and David J. ELLAR†[2]

*Department of Chemistry, University of Cambridge, Lensfield Road, Cambridge CB2 1EW, U.K., and †Department of Biochemistry, University of Cambridge, 80 Tennis Court Road, Cambridge CB2 1GA, U.K.

The *Bacillus thuringiensis* Cry1Ac δ-endotoxin was shown to bind in a biphasic manner to *Manduca sexta* aminopeptidase N (APN) present in a novel model membrane. Surface plasmon resonance analysis allowed the quantification of toxin binding to *M. sexta* APN in a supported lipid monolayer. The initial binding was rapid and reversible, with an affinity constant of 110 nM. The second phase was slower and resulted in an overall affinity constant of 3.0 nM. Reagents used to disrupt protein–protein interactions did not dissociate the toxin after high-affinity binding was attained. The initial association between Cry1Ac and APN was inhibited by the sugar GalNAc, but the higher-affinity state was resistant to GalNAc-induced dissociation. The results suggest that after binding to *M. sexta* APN, the Cry1Ac toxin undergoes a rate-limiting step leading to a high-affinity state. A site-directed Cry1Ac mutant, N135Q, exhibited a similar initial binding affinity for APN but did not show the second slower phase. This inability to form an irreversible association with the APN-lipid monolayer helps explain the lack of toxicity of this protein towards *M. sexta* larvae and its deficient membrane-permeabilizing activity on *M. sexta* midgut brush border membrane vesicles.

INTRODUCTION

Cry toxins are a family of proteins produced by the bacterium *Bacillus thuringiensis*, many of which have insecticidal properties ([1]; Cry toxins named in accordance with revised nomenclature: WWW site http://www.biols.susx.ac.uk/Home/Neil_Crickmore/Bt/]. They form intracellular inclusions during sporulation, known as δ-endotoxins, which are released along with the bacterial spore on cell lysis. The δ-endotoxin inclusions are composed of one or more Cry toxins in the form of inactive protoxins. After ingestion by a susceptible insect the inclusion is solubilized and the protoxins are activated proteolytically within the insect midgut [2]. After activation, the Cry toxin binds to specific receptors located on the midgut epithelial cell membrane [3–5], subsequently inducing a membrane permeability change [6,7] that leads to cell death by colloid osmotic lysis [8].

A putative receptor for the Cry1Ac toxin has been identified as aminopeptidase N (APN) in four lepidopteran insects [9–13]. APN was also identified as a receptor for Cry1Aa in *Bombyx mori* (silkworm) [14], and for Cry1C and Cry1Ab in *Manduca sexta* (tobacco hornworm) [15,16]. The APN proteins in *M. sexta* are distinct, forming a family of related putative toxin receptors. Vadlamudi et al. [17] reported that Cry1Ab also binds to a 210 kDa cadherin-like protein in *M. sexta*. A protein complex isolated from *M. sexta*, containing the Cry1Ac-binding 120 kDa APN and possibly associated lipid, was shown to lower the amount of Cry1Ac required to induce ion flux across a membrane when incorporated into phospholipid vesicles [10] or planar lipid bilayers [18]. Although this demonstrated a direct role for this mixture of proteins in toxin activity, in most cases it remains to be shown whether the putative receptor actually has a role in the activity of Cry toxins.

Recently the technique of surface plasmon resonance (SPR) has been used to study Cry toxin binding to both insect midgut brush border membrane vesicles (BBMV) and a purified toxin receptor [19,20]. With this technique, ligands (receptor, BBMV or toxin) are immobilized on a sensor chip and the interaction of a specific analyte with the immobilized ligand can be followed in real time. Changes in the measured refractive index as an analyte binds to the ligand, given in response units (RU), are proportional to the amount of material in the immediate vicinity of the sensor surface [21]. By using these changes in refractive index, the affinity of the binding event can be calculated from an analysis of the resultant binding curve. The results obtained have provided an interesting comparison with previous Cry toxin-binding studies.

The affinity constant (K_d) obtained by SPR analysis of the Cry1Ac interaction with APN isolated from *M. sexta* was two orders of magnitude lower than that reported from equilibrium binding studies with Cry1Ac and intact *M. sexta* BBMV [4,19]. The SPR experiments used APN covalently attached to a carboxymethylated dextran matrix, in the absence of other membrane components. It was suggested that the presence of other molecules in BBMV, particularly lipid, might be responsible for the observed differences [19]. The fact that Cry toxin binding to BBMV from susceptible insects is quickly irreversible [22], indicating toxin insertion into the membrane, could account for the higher affinity of Cry1Ac for intact BBMV. Indeed, in a number of studies it is the irreversible binding step that has been shown to be correlated with toxin activity *in vivo* [23,24].

In the study described here we have employed SPR analysis with a hydrophobic association sensor chip (Biacore AB), which consists of a self-assembled monolayer of alkane thiol on a gold

Abbreviations used: APN, aminopeptidase N; BBMV, brush border membrane vesicles; Caps, 3-(cyclohexylamino)propane-1-sulphonic acid; Ches, 2-(cyclohexylamino)ethanesulphonic acid; RU, response unit; SPR, surface plasmon resonance.

[1] Present address: Institute of Biotechnology, University of Cambridge, Tennis Court Road, Cambridge CB2 1QT, U.K.

[2] To whom correspondence should be addressed (e-mail dje1@mole.bio.cam.ac.uk).

film. Lipid vesicles are spontaneously absorbed on the alkane surface to form a supported lipid monolayer [25] that chemically and physically resembles the surface of a cell membrane. The phenomenon of SPR can then be exploited to study interactions with lipophilic ligands inserted into the monolayer, mimicking the membrane environment. This technique was used to investigate the interaction of Cry1Ac with intact APN purified from *M. sexta*. The results obtained help to explain the differences seen between previous binding studies with either the purified APN [19] or intact BBMV [4,26].

EXPERIMENTAL

Purification and activation of Cry1Ac

B. thuringiensis subsp. *kurstaki* HD73, which synthesizes a single Cry1Ac protoxin inclusion [1], was obtained from USDA Northern Regional Research Laboratories (Peoria, IL, U.S.A.). A Cry1Ac mutant protoxin, N135Q, was constructed and the protein was expressed in the acrystalliferous strain *B. thuringiensis* subsp. *israelensis* IPS-78/11 by the method described by Smedley and Ellar [27]. Both *B. thuringiensis* subsp. *israelensis* IPS-78/11 expressing the wild-type or N135Q mutant and *B. thuringiensis* subsp. *kurstaki* HD73 were grown as described for *Bacillus megaterium* KM [28]. Purification of crystals, solubilization, activation with *Pieris brassicae* gut extract and SDS/PAGE analysis were performed as described previously [7]. Activation of soluble Cry1Ac with trypsin was performed with 1:10 (w/w) trypsin (Sigma)/toxin at 37 °C for 1 h followed by the addition of a further 1:10 (w/w) trypsin/toxin and 10% (v/v) 2 M Tris/HCl, pH 7.5, and incubation overnight at 37 °C.

M. sexta midgut BBMV preparation and APN purification

M. sexta eggs were obtained from Dr. S. Reynolds (School of Biological Sciences, University of Bath, Bath, Avon, U.K.) and the larvae were reared on an artificial diet [29]. BBMV were isolated by the method of Wolfersberger et al. [30]. The final BBMV preparation was resuspended in 10 mM Tris/HCl/150 mM KCl/1 mM EGTA/0.1 mM PMSF (pH 8) and stored at −70 °C. A Cry1Ac-binding protein, APN, found in *M. sexta* BBMV was purified by protoxin affinity chromatography by the method of Knight et al. [9]. After affinity column purification APN was concentrated and the buffer was exchanged for 100 mM Tris/HCl, pH 8.5, with a Centricon-30 ultrafiltration device (Amicon). Both the BBMV and APN protein concentrations were quantified by the method of Bradford [31] with a Bio-Rad protein assay dye reagent.

BBMV permeability assay

BBMV solute permeability was studied with the use of a light-scattering assay described by Carroll and Ellar [7], with minor modifications. BBMV at 0.2 mg/ml in 10 mM 2-(cyclohexylamino)ethanesulphonic acid (Ches)/KOH/0.1% BSA (pH 9) were mixed 1:1 (v/v) with hyperosmotic 150 mM KCl prepared in the same Ches buffer, pH 9, and changes were monitored by 90° light-scattering at 450 nm. Quantification of the activated toxin preparations used in these assays was performed by gel-scanning densitometry as described previously [32].

M. sexta bioassays

Freshly hatched larvae, reared from eggs as described above, were assayed with solubilized protoxin preparations. The solubilized protoxin concentration was determined by the method of Bradford [31] with a Bio-Rad protein assay dye reagent. The toxin was then diluted to the desired concentration in PBS (Oxoid) and 20 μl was layered on 1 cm^2 discs of artificial diet. One larva was placed on each disc. Mortality was assessed after 5 days, and with results from three separate experiments LC_{50} values were determined by probit analysis [33] with the computer program of Lieberman [34].

Preparation of vesicles

Small unilamellar vesicles were prepared in 100 mM phosphate buffer (100 mM Na_2HPO_4/NaH_2PO_4, pH 7.4) by extrusion. Egg-yolk L-α-phosphatidylcholine (Sigma) (128 mg, 160 μmol) was dissolved in 10 ml of ethanol-free chloroform in a 100 ml round-bottomed flask. The lipid was deposited as a thin film by removal of the solvent under reduced pressure on a rotary evaporator, then dried under high vacuum for 2 h. Phosphate buffer was then added to give a 20 mM suspension. The lipid was shaken for 30 min, then passed 17 times through a 50 nm polycarbonate filter in an Avestin Lipofast Basic® extrusion apparatus to give a translucent solution. Vesicles containing surface Cry1Ac receptor were prepared by shaking an aliquot of 500 μM vesicles with 100 nM APN for 5 min.

Formation of lipid monolayers

Vesicles at 500 μM were loaded on a hydrophobic association (HPA) sensor chip in a Biacore 2000 biosensor (Biacore AB) as described previously [35]. The eluent buffer was then changed to 3-(cyclohexylamino)propane-1-sulphonic acid (Caps)-buffered saline [10 mM Caps/KOH/150 mM NaCl (pH 10)], which was used for all subsequent binding experiments. Buffer passed over the monolayer at 20 μl/min for 18 h resulted in a baseline drift of less than 0.3 RU/min. The HPA sensor chip contained four flow cells of dimensions 2.4 mm × 0.5 mm × 0.05 mm (length × width × height) with a probing spot for the SPR signal of approx. 0.26 mm^2.

SPR binding assay

Activated Cry1Ac toxin was separated from low-molecular-mass digest products with a micro Bio-spin 30 chromatography column (Bio-Rad) in accordance with the manufacturer's instructions. This step also exchanged the toxin incubation buffer with Caps-buffered saline, pH 10. Quantification of the activated toxin preparations was performed by measuring UV absorbance at 280 nm [36] and corrected with control enzyme preparations. *B. thuringiensis* subsp. *kurstaki* HD73 wild-type Cry1Ac and *B. thuringiensis* subsp. *israelensis* IPS-78/11-expressed N135Q proteins were used. Toxins were diluted in Caps-buffered saline, pH 10, from 500 to 16 nM and were passed serially at a flow rate of 20 μl/min over a flow cell containing a lipid monolayer alone, then over a flow cell containing lipid and APN receptor. The sample solution was then replaced by Caps-buffered saline and the toxin–receptor complex was allowed to dissociate for 4 min. All assays were performed at 25 °C.

Inhibition of Cry1Ac binding

A 300 nM stock solution of insect gut extract-activated Cry1Ac was preincubated with various concentrations of GalNAc and GlcNAc in Caps-buffered saline, pH 10, at 0 °C for 30 min before the SPR binding assay. The maximum binding level to an APN-lipid monolayer was determined in the absence of inhibitor. Data from the flow cell containing lipid alone were subtracted

from corresponding data obtained from the receptor-containing flow cell to correct for the bulk refractive index changes due to the large amount of inhibitor present in the sample. The K_d value for competitive inhibition was determined from a non-linear least-squares fit of the inhibitor concentration plotted against percentage inhibition. The ability of the inhibitor to dissociate stably bound Cry1Ac was tested by injection of 40 μl of a 100 mM GalNAc solution in Caps-buffered saline, pH 10, after a 60 μl injection of 500 nM Cry1Ac across an APN-lipid monolayer.

SPR data analysis

Data were prepared for analysis by subtracting the average response recorded 20 s before injection and adjusting the time of each injection to zero. Data from the flow cell containing lipid alone were subtracted from corresponding data obtained from the receptor containing flow cell to correct for bulk refractive index changes. Analysis was performed with BIAEVAL 3.0 global analysis software based on algorithms for numerical integration [37]. Both a simple bimolecular association model and a complex biphasic model were employed.

For the simple bimolecular association the process was assumed to be pseudo-first-order with no interaction between separate receptor molecules. The association and dissociation rates, k_a and k_d, for the formation of a homogeneous binary complex of analyte A and ligand B in solution are given by:

$$\begin{array}{lccccc} & \mathrm{A} & + & \mathrm{B} & \overset{k_a}{\underset{k_d}{\rightleftharpoons}} & \mathrm{AB} \\ t=0: & A_0 & & B_0 & & 0 \\ t=t: & A_0-AB_t & & B_0-AB_t & & AB_t \end{array} \quad (1)$$

thus:

$$\mathrm{d[AB]}/\mathrm{d}t = k_a[\mathrm{A}][\mathrm{B}] - k_d[\mathrm{AB}]$$

In the SPR flow cell, the analyte is being continually added to and removed from the system so the concentration will remain at the initial value, C. The total amount of ligand present is expressed in terms of R_{max}, the maximum possible response. The amount of complex formed is proportional to R_t, the observed response. Thus after a time t the concentration of analyte will still be C and the amount of free ligand will be given by $R_{max} - R_t$.

In the flow cell:

$$\begin{array}{lccccc} & \mathrm{A} & + & \mathrm{B} & \overset{k_a}{\underset{k_d}{\rightleftharpoons}} & \mathrm{AB} \\ t=0: & C & & R_{max} & & 0 \\ t=t: & C & & R_{max}-\mathrm{R}_t & & R_t \end{array} \quad (2)$$

thus:

$$\mathrm{d}R/\mathrm{d}t = k_a C(R_{max} - R_t) - k_d R_t$$

For the more complex biphasic model, the association rates, k_{a1} and k_{a2}, and the dissociation rates, k_{d1} and k_{d2}, are described by:

$$\begin{array}{lccccc} & \mathrm{A}+ & & \mathrm{B} & \overset{k_{a1}}{\underset{k_{d1}}{\rightleftharpoons}} \mathrm{AB} & \overset{k_{a2}}{\underset{k_{d2}}{\rightleftharpoons}} \mathrm{AB^*} \\ t=0: & C & & R_{max} & 0 & 0 \\ t=t: & C & & R_{max}-R_1-R_2 & R_1 & R_2 \end{array} \quad (3)$$

thus:

$$\mathrm{d}R_1/\mathrm{d}t = k_{a1}C(R_{max} - R_1 - R_2) - k_{d1}R_1 - k_{a2}R_1 - k_{a2}R_1 + k_{d2}R_2$$

$$\mathrm{d}R_2/\mathrm{d}t = k_{a2}R_1 - k_{d2}R_2$$

with both R_1, the response due to AB, and R_2, the response due to AB*, contributing to the total observed response.

RESULTS

Toxicity *in vivo*

The LC_{50} for wild-type Cry1Ac protoxin against newly hatched *M. sexta* larvae was 14.4 ng/cm² (95% confidence interval 12.0–18.9 ng/cm²). No significant difference was seen between wild-type protoxin isolated from *B. thuringiensis* subsp. *kurstaki* HD73 and the cloned wild-type protein expressed in *B. thuringiensis* subsp. *israelensis* IPS-78/11 (results not shown). In contrast with the wild-type activity the Cry1Ac mutant N135Q was non-toxic at concentrations up to 200 ng/cm².

BBMV-permeabilizing activity

The BBMV-permeabilizing activity of the activated toxins was tested by using a light-scattering assay (Figure 1). The light-scattering signal recovery observed in the presence of wild-type Cry1Ac toxin (Figure 1A, traces a and b) resulted from the entry of KCl through a toxin-induced membrane lesion, followed by water. However, the Cry1Ac mutant N135Q failed to alter the permeability of *M. sexta* BBMV for KCl (Figure 1A, trace c).

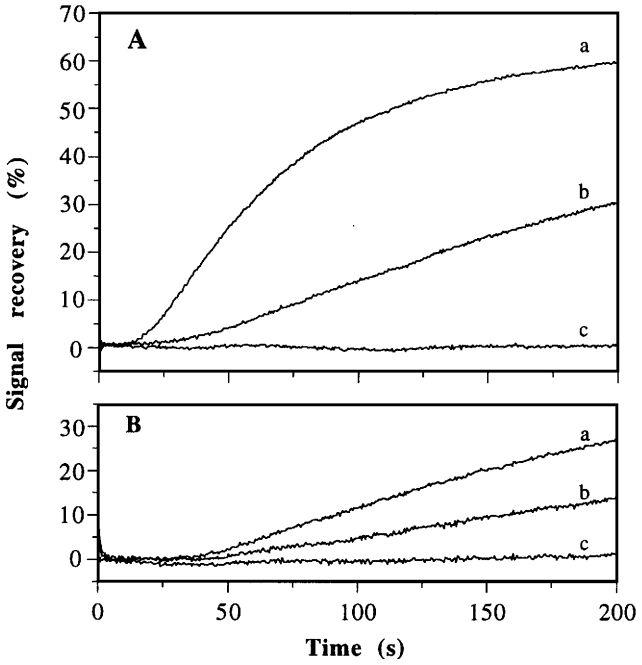

Figure 1 Cry1Ac-induced signal recovery in *M. sexta* BBMV swelling after mixing with hyperosmotic KCl: toxin mixing assay

(**A**) BBMV (0.2 mg/ml) equilibrated with 10 mM Ches/KOH/0.1% (w/v) BSA (pH 9.0) were mixed with 10 mM Ches/KOH/0.1% (w/v) BSA/150 mM KCl (pH 9.0) containing Cry1Ac toxin, with a stopped-flow spectrometer at 20–21 °C. Trace a, wild-type Cry1Ac (59 pmol/mg of BBMV); trace b, wild-type Cry1Ac (12 pmol/mg of BBMV); trace c, Cry1Ac mutant N135Q (416 pmol/mg of BBMV). Re-swelling was followed as the change in 90° light scattering at 450 nm over 200 s. Each trace represents the average of two separate determinations corrected for control changes, showing light-scattering signal recoveries relative to the signal change observed for the control. (**B**) Conditions as (**A**). Trace a, wild-type Cry1Ac (12 pmol/mg of BBMV); trace b, wild-type Cry1Ac (12 pmol/mg of BBMV) plus Cry1Ac mutant N135Q (21 pmol/mg of BBMV); trace c, wild-type Cry1Ac (12 pmol/mg of BBMV) plus Cry1Ac mutant N135Q (416 pmol/mg of BBMV). Both wild-type and N135Q proteins were those expressed in *B. thuringiensis* subsp. *israelensis* IPS-78/11.

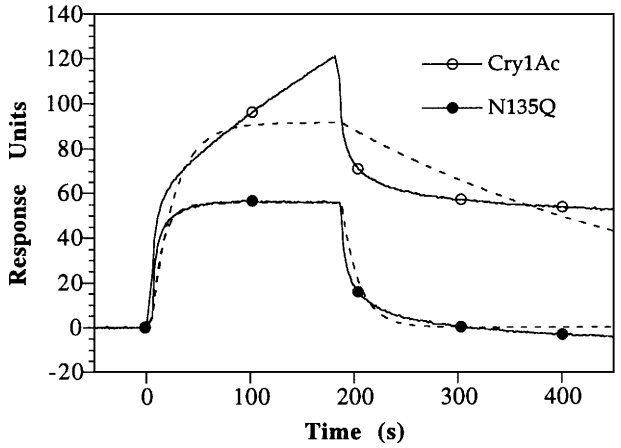

Figure 2 Binding of wild-type Cry1Ac and mutant N135Q toxin to an APN-lipid monolayer

Injections of 250 nM toxin preparations over an APN-lipid surface formed from liposomes composed of 500 μM egg-yolk L-α-phosphatidylcholine and 100 nM APN (solid lines). The eluent buffer was 10 mM Caps/150 mM NaCl/KOH (pH 10). The flow rate was 20 μl/min and the temperature was 25 °C. At the end of the injection the toxin solution was replaced by buffer alone to allow the complexes to dissociate. Data from the flow cell containing lipid alone were subtracted from corresponding data obtained from the receptor-containing flow cell to correct for the bulk refractive index changes. The binding curves were fitted to a simple bimolecular binding algorithm (broken lines) [37] with a χ^2 of 109 for wild-type Cry1Ac and a χ^2 of 6.7 for N135Q.

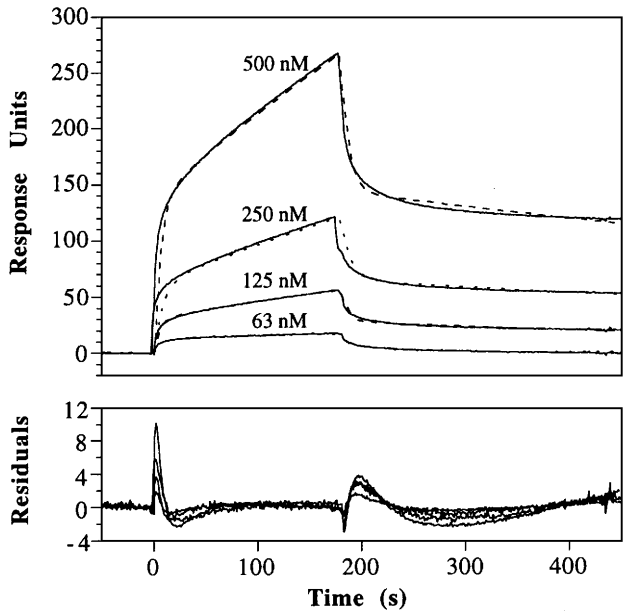

Figure 3 Binding of Cry1Ac at various concentrations to an APN-lipid monolayer

Injections of Cry1Ac at various concentrations over an APN-lipid surface formed from liposomes composed of 500 μM egg-yolk L-α-phosphatidylcholine and 100 nM APN. The eluent buffer was 10 mM Caps/150 mM NaCl/KOH (pH 10). The flow rate was 20 μl/min and the temperature was 25 °C. The experimental data are for the binding of Cry1Ac to an APN-lipid monolayer corrected for bulk refractive index changes by the subtraction of control data for toxin passed over a lipid monolayer alone (solid lines). The data set were globally fitted to the biphasic model described in the Discussion section (broken lines) with a χ^2 of 6.1.

Despite a lack of permeabilizing activity, preliminary experiments demonstrated that the presence of the mutant N135Q inhibited the action of wild-type Cry1Ac toxin (Figure 1B, traces b and c). In addition, N135Q was shown to bind to a 120 kDa *M. sexta* BBMV protein and also to a purified APN preparation in a similar manner to that of wild-type Cry1Ac with toxin–ligand immunoblotting (results not shown).

SPR binding assay

APN was successfully deposited in a lipid monolayer when APN was shaken in an aqueous suspension of phosphatidylcholine vesicles and this preparation was layered on the sensor chip. Typically approx. 1500 RU of lipid and approx. 2100 RU of lipid-APN was deposited. As the measured response at the surface is proportional to the associated mass [21], this corresponds to a lipid/receptor ratio of 2.5/1 (w/w) or 375/1 (mol/mol). Specific binding of protease-activated toxins to the APN-lipid monolayer was observed with very little interaction of toxin preparations with the lipid surface alone. No binding of the protease controls to the APN-lipid monolayer was observed (results not shown). N135Q toxin associated rapidly with, and dissociated rapidly from, the APN-lipid monolayer (Figure 2). In contrast, wild-type Cry1Ac toxin preparations associated with high affinity to form a new, stable baseline (Figures 2 and 3) that was unaffected by injections of 10 mM HCl, 10 mM glycine, pH 2.0, 10 mM NaOH or 3 M KCl (results not shown).

Wild-type toxin thus associated with the surface was also not displaced by injection of 100 mM GalNAc (Figure 4), which was shown to completely inhibit binding to the receptor after preincubation with toxin (Figure 5). Complete inhibition of binding of wild-type Cry1Ac toxin to APN was observed after preincubation with 40 mM GalNAc. No inhibition occurred with the epimeric GlcNAc. Titration of GalNAc with a constant amount of the toxin gave a K_d value for competitive inhibition of toxin binding with GalNAc of 4.6 mM.

The reversible association of N135Q and the essentially irreversible association of wild-type Cry1Ac suggest that,

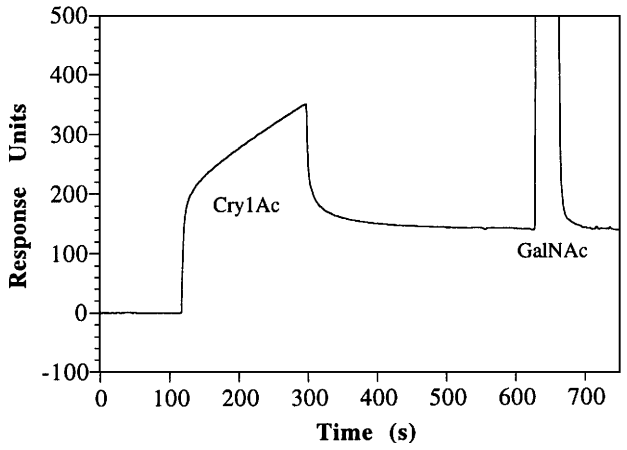

Figure 4 Injection of wild-type Cry1Ac toxin across an APN-lipid monolayer followed by an injection of GalNAc

Shown is the result of successive injections of Cry1Ac toxin at 500 nM and the competitive inhibitor GalNAc at 100 mM across an APN-lipid monolayer formed from liposomes composed of 500 μM egg-yolk L-α-phosphatidylcholine and 100 nM APN. The eluent buffer was 10 mM Caps/150 mM NaCl/KOH (pH 10). The flow rate was 20 μl/min and the temperature was 25 °C.

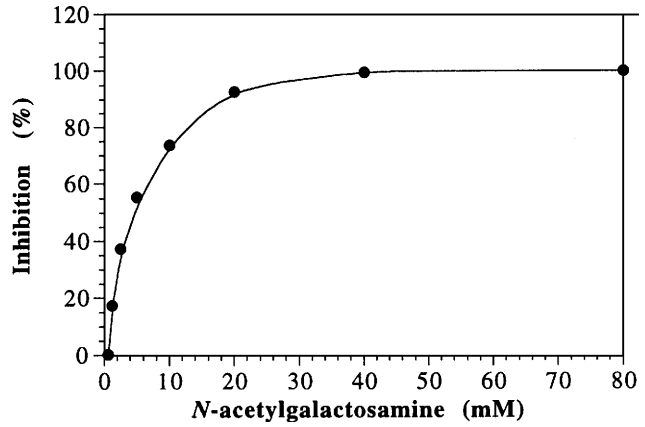

Figure 5 Inhibition of Cry1Ac binding by GalNAc

A 300 nM stock solution of wild-type Cry1Ac toxin was incubated with various concentrations of GalNAc before injection over an APN-lipid monolayer formed from liposomes composed of 500 μM egg-yolk L-α-phosphatidylcholine and 100 nM APN. The eluent buffer was 10 mM Caps/150 mM NaCl/KOH (pH 10). The flow rate was 20 μl/min and the temperature was 25 °C. The maximum binding level corrected for bulk refractive index changes caused by the high inhibitor concentration was determined, and the level of inhibition compared with this response level was plotted as a function of inhibitor concentration.

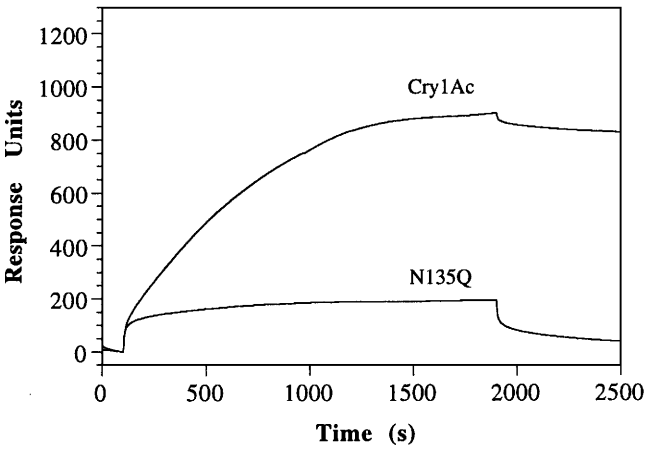

Figure 6 Binding of wild-type Cry1Ac and N135Q at 125 nM over 30 min to a APN-lipid monolayer

Shown are the results of extended injections of toxins over an APN-lipid monolayer corrected for bulk refractive index changes. Wild-type Cry1Ac at 125 nM was injected at a flow rate of 10 μl/min for 30 min over an APN-lipid monolayer formed from liposomes composed of 500 μM egg-yolk L-α-phosphatidylcholine and 100 nM APN. The monolayer was then removed by an injection of 40 mM octyl-D-glucoside, the surface was reloaded with APN-liposomes, and N135Q toxin at 125 nM was injected across the surface at a flow rate of 10 μl/min. The eluent buffer was 10 mM Caps/150 mM NaCl/KOH (pH 10); the temperature was 25 °C.

Table 1 Association rate constants (k_{a1}) for the binding of Cry1Ac to an APN-lipid monolayer at various flow rates

	$10^{-5} \times k_{a1}$ ($M^{-1}s \cdot^{-1}$)					
Flow (μl/min) ...	2	5	10	20	50	100
	4.50	4.61	4.68	4.74	4.80	4.82

Table 2 Measured rate and affinity constants for binding of purified toxin preparations with an APN-lipid monolayer

K_1 is defined as k_{d1}/k_{a1} for the reversible binding event and K_2 as k_{d2}/k_{a2} for the conformational change event. The apparent overall affinity, K_d, is defined as K_1K_2. Data for the N135Q APN-lipid monolayer were fitted to a simple, bimolecular association to give a single association and dissociation constant.

Toxin assay	k_a	k_d	Affinity
Cry1Ac APN-lipid monolayer	$k_{a1} = 4.7 \times 10^5$ $M^{-1} \cdot s^{-1}$ $k_{a2} = 6.1 \times 10^{-3}$ s^{-1}	$k_{d1} = 5.2 \times 10^{-2}$ s^{-1} $k_{d2} = 1.7 \times 10^{-4}$ s^{-1}	$K_1 = 110$ nM $K_2 = 0.028$ $K_d = 3.0$ nM
N135Q APN-lipid monolayer	5.1×10^5 $M^{-1} \cdot s^{-1}$	5.3×10^{-2} s^{-1}	$K_d = 104$ nM
Cry1Ac-solubilized APN*	9.2×10^4 $M^{-1} \cdot s^{-1}$	8.8×10^{-3} s^{-1}	$K_d = 95$ nM

* From [19].

whereas both toxins bind to the receptor, only the latter associates with the lipid monolayer with extremely high affinity. The contrasting behaviour of the two toxins can be seen clearly from a 30 min injection (Figure 6).

The amount of toxin associating with high affinity remained stable for 24 h after activation with gut proteases when toxin was stored at 0 °C. After this time the ability of the toxin to form the high-affinity state decreased slowly, although the toxin still bound reversibly to the receptor up to 80 h after activation (results not shown).

SPR data analysis

Association rate constants measured at various flow rates showed only slight variation from the mean (Table 1). This indicates that, at the planar monolayer surface, association was not unduly limited by mass transport [38] from the bulk solution. Table 2 shows measured rate and affinity constants for toxin binding to the APN-lipid monolayer. Data for the binding of N135Q, corrected for bulk refractive index change, fitted well to a simple bimolecular association model (Figure 2; $\chi^2 = 6.7$ for single fit) giving a K_d of 104 nM (Table 2). In contrast, wild-type Cry1Ac bound to the receptor in a biphasic manner (Figure 3) and did not fit well to a simple bimolecular association model (Figure 2; $\chi^2 = 109$ for single fit). Data for wild-type Cry1Ac binding were therefore fitted with the BIAEVAL 3.0 analysis package to a model describing an initial fast binding event followed by a slower, irreversible step (see the Experimental section). A global fitting algorithm [39], which improves the robustness of the fitting procedure by simultaneously fitting all binding curves in the data set, was used. Global fitting contributes greatly to the stability of the fitting procedure for complex models with many variables, and also reflects many physical interaction systems more faithfully (a set of data for the same interaction at different analyte concentrations should *a priori* have identical rate constants). The standard errors for kinetic constants calculated gave an overall χ^2 of 6.1 for the simultaneous fitting of four binding curves (Figure 3). K_1, which describes the affinity of the initial toxin binding event, was calculated to be 110 nM; K_2, which describes the second slower event, was calculated to be 0.028 (Table 2). The latter constant is dimensionless as it describes a unimolecular event that is concentration-independent. K_d, the

overall affinity constant defined as the product of K_1 and K_2, was calculated to be 3.0 nM.

DISCUSSION

If programmes aimed at improving toxin potency and combating the development of toxin resistance are to be realized, an understanding of the mechanism of action of *B. thuringiensis* Cry toxins is required. Two steps in this mechanism are receptor binding followed by membrane permeabilization. The Cry1Ac toxin has been shown to bind to APN in the midgut brush border membrane of *M. sexta* [9,10] and to induce a membrane permeability change in *M. sexta* BBMV [6,7]. By using SPR analysis of a supported lipid monolayer we have further dissected the steps of Cry1Ac–APN binding and membrane association. After an initial reversible binding with APN, Cry1Ac was observed to form an effectively irreversible complex with the lipid monolayer. Kinetic analysis of toxin binding with this novel model membrane system enables the examination of the effects of mutations generated in these toxin proteins.

Cry toxins are composed of three domains [40,41]. Functions have been tentatively assigned to these domains, domain I being involved in membrane channel formation, domain II in receptor binding and domain III in both receptor binding and influencing channel formation, although the exact distribution of function might be more complex [42]. The Cry1Ac mutant N135Q used in this study contains a point mutation in α-helix 4 of domain I. This protein bound to a 120 kDa component of *M. sexta* BBMV, previously identified as APN [9,10] and to an APN preparation isolated from this tissue, in a similar manner to that of wild-type toxin (results not shown). However, unlike the wild-type toxin, N135Q was not active against *M. sexta* larvae and did not possess the ability to permeabilize *M. sexta* BBMV (Figure 1). We have demonstrated that although N135Q binds to *M. sexta* APN it does not readily associate irreversibly with the receptor–membrane complex, helping to explain the lack of toxicity exhibited by this protein. Both N135Q and wild-type Cry1Ac bind to APN with similar initial association rates, then only Cry1Ac binds further at a much slower rate (Table 2). This suggests that both toxins bind initially to APN in a similar manner and only the latter then undergoes a second step resulting in the toxin forming a high-affinity association with the APN-lipid monolayer. Toxin binding followed by a conformational change and membrane insertion is a proposed mechanism for pore formation by Cry toxin [40].

In a similar manner to that of N135Q, mutations in α-helix 5 of both Cry1Ac [43] and Cry1Aa [44] do not alter receptor recognition, but decrease the ability of the toxin to permeabilize target membranes. Whether this is due to a deleterious effect on irreversible binding or to defective pore formation was not determined. Certain point mutations in or near loop regions between helices in domain I of Cry1Ab (A92E and Y153D) had the same properties, namely unaltered initial binding but decreased activity [45]. However, these mutants were also shown to exhibit decreased irreversible binding. It was proposed that these mutations were on the membrane proximal surface of domain I, the introduced charged groups inhibiting effective membrane association. The conserved mutation in N135Q is situated within α-helix 4 and must act differently in impeding the change required for high-affinity binding to the membrane.

The calculated rate constants (Table 2) for Cry1Ac toxin binding to the APN-lipid monolayer chip show that the initial binding event is fast and the subsequent step is slow and rate-limiting. The initial dissociation of bound toxin is also very fast and the subsequent dissociation of residual material is very slow. Masson et al. [19] reported a K_d of 95 nM for the Cry1Ac interaction with *M. sexta* APN in the absence of other membrane components. This is much lower than the K_d range, 0.2–1.6 nM, previously reported for radiolabelled Cry1Ac toxin interactions with *M. sexta* BBMV [4,26] but similar to the affinity constant (K_1) of 110 nM reported in the present study for the initial reversible association. This suggests that the value reported by Masson et al. [19] is a measure of the affinity of the initial binding event only. We have shown that the wild-type Cry1Ac toxin associated with an APN-lipid monolayer in a biphasic manner, the second step being effectively irreversible (Figure 3). The calculated overall K_d was 3.0 nM (Table 2), which approaches the K_d range noted above for interactions of radiolabelled Cry1Ac toxin with *M. sexta* BBMV. Therefore the irreversible association dominates values obtained from toxin equilibrium binding studies with BBMV, and the reversible association dominates values with solubilized APN.

The Cry1Ac binding APN in *M. sexta* is a glycosylated, glycosylphosphatidylinositol (GPI)-anchored membrane protein [46,47]. The APN preparation used by Masson et al. [19] was treated with phosphatidylinositol phospholipase C, which removed the GPI anchor, in contrast with the intact APN used in the present study. Recently, binding of Cry1-type toxins to a protein complex isolated from *M. sexta*, containing the intact APN, was studied with SPR [18]. However, a quantitative analysis was not attempted, preventing a comparison with our data. GalNAc has been implicated as the putative toxin recognition element on APN for Cry1Ac [48]. A K_d of 4.6 mM was determined for the competitive inhibition of Cry1Ac–APN association with GalNAc (Figure 5). This value compares favourably with the value (5 mM) reported in the literature for the phosphatidylinositol phospholipase C-treated APN [19].

When an extended injection of wild-type Cry1Ac was passed across a surface containing 615 RU of receptor, approx. 900 RU of toxin bound to the monolayer (Figure 6). These signal levels correspond [21] to calculated surface densities of 0.47 and 1.27 pmol/cm^2 for APN and Cry1Ac respectively and therefore a stoichiometry of approximately three molecules of toxin to one molecule of APN. This implies that either the APN possesses more than one binding site or that on forming the higher-affinity state the toxin releases the binding site on APN, allowing it to bind more toxin. The former possibility is not favoured by our data because if the toxin were merely binding to multiple binding sites then all of the bound material should still be dissociated with the competitor GalNAc. However, the possibility of binding to more than one site on APN [19], each leading to a higher affinity state for the toxin, cannot be discounted.

The release of toxin from the receptor after binding is described by eqn. (4) and implies a turnover capacity for the receptor. However, because the amount of membrane-associated toxin reaches a maximum after an extended injection (Figure 6), the data were fitted by using the simpler model described in eqn. (5), in which a maximum binding level is attained:

$$A + B \underset{k_{d1}}{\overset{k_{a1}}{\rightleftharpoons}} AB \underset{k_{d2}}{\overset{k_{a2}}{\rightleftharpoons}} A^* + B \quad (4)$$

$$A + B \underset{k_{d1}}{\overset{k_{a1}}{\rightleftharpoons}} AB \underset{k_{d2}}{\overset{k_{a2}}{\rightleftharpoons}} AB^* \quad (5)$$

The experimental data, in particular the resistance of the bound toxin to GalNAc-induced dissociation (Figure 4), implies that toxin in the high-affinity complex is integrally associated with the lipid monolayer. However, we accept that this model might not describe accurately the oligomeric nature of the

toxin–receptor–membrane complex and that the lipid monolayer is not a completely accurate representation of a natural membrane. It is possible that there is a limit imposed by steric constraints of packing in the monolayer.

Binding of Cry toxin to insect midgut BBMV has generally been analysed by assuming a simple one-step reversible association. However, very strong binding to target membranes, presumably resulting from toxin insertion into the bilayer, was shown to follow the initial binding event [22] and to be an important determinant of activity *in vivo* [23]. Liang et al. [24] began to analyse Cry toxin binding quantitatively in terms of a two-step model, the first step being a low-affinity reversible interaction with the receptor, quickly followed by a higher-affinity, effectively irreversible, association with the target membrane. This approach demonstrated that the activity of different Cry1A toxins against *Lymantria dispar* was correlated with the high-affinity binding rate constant. By using a different experimental system we have analysed the two steps of receptor binding and membrane association. *M. sexta* APN in a membrane environment promotes Cry1Ac association with affinities comparable to that observed with target *M. sexta* midgut membranes. Mutations in the toxin that block the transition from initial receptor binding to the high-affinity state render the toxin inactive. The calculated affinity constants, K_1 and K_d, for wild-type Cry1Ac toxin association with the APN-lipid monolayer (Table 2) describe the affinity of the initial reversible APN-binding step and the higher-affinity membrane-associated state respectively. The results also suggest that after toxin binding reaches the high-affinity state, the binding site on the receptor is free to bind further toxin.

We thank Dr. N. Crickmore for his help in constructing the mutant N135Q, Dr. P. Koni for the sequencing of this mutant, and Dr. S. Kumar (Biacore AB) for access to the Biacore 2000 instrument. This work was supported by EPSRC, U.K. (M.A.C. and D.H.W.) and BBSRC, U.K. (J.C., E.R.T. and D.J.E.).

REFERENCES

1 Höfte, H. and Whiteley, H. R. (1989) Microbiol. Rev. **53**, 242–255
2 Knowles, B. H. (1994) Adv. Insect Physiol. **24**, 275–308
3 Hofmann, C., Vanderbruggen, H., Höfte, H., Van Rie, J., Jansens, S. and Van Mellaert, H. (1988) Proc. Natl. Acad. Sci. U.S.A. **85**, 7844–7848
4 Van Rie, J., Jansens, S., Höfte, H., Degheele, D. and Van Mellaert, H. (1989) Eur. J. Biochem. **186**, 239–247
5 Martínez-Ramírez, A. C. and Real, M. D. (1996) Pestic. Biochem. Physiol. **54**, 115–122
6 Wolfersberger, M. G. (1989) Arch. Insect Biochem. Physiol. **12**, 267–277
7 Carroll, J. and Ellar, D. J. (1993) Eur. J. Biochem. **214**, 771–778
8 Knowles, B. H. and Ellar, D. J. (1987) Biochim. Biophys. Acta **924**, 509–518
9 Knight, P. J. K., Crickmore, N. and Ellar, D. J. (1994) Mol. Microbiol. **11**, 429–436
10 Sangadala, S., Walters, F. S., English, L. H. and Adang, M. J. (1994) J. Biol. Chem. **269**, 10088–10092
11 Gill, S. S., Cowles, E. A. and Francis, V. (1995) J. Biol. Chem. **270**, 27277–27282
12 Valaitis, A. P., Lee, M. K., Rajamohan, F. and Dean, D. H. (1995) Insect Biochem. Molec. Biol. **25**, 1143–1151
13 Luo, K., Tabashnik, B. E. and Adang, M. J. (1997) Appl. Environ. Microbiol. **63**, 1024–1027
14 Yaoi, K., Kadotani, T., Kuwana, H., Shinkawa, A., Takahashi, T., Iwahana, H. and Sato, R. (1997) Eur. J. Biochem. **246**, 652–657
15 Luo, K., Lu, Y.-J. and Adang, M. J. (1996) Insect Biochem. Mol. Biol. **26**, 783–791
16 Denolf, P., Hendrickx, K., Van Damme, J., Jansens, S., Peferoen, M., Degheele, D. and Van Rie, J. (1997) Eur. J. Biochem. **248**, 748–761
17 Vadlamudi, R. K., Weber, E., Ji, I., Ji, T. H. and Bulla, Jr., L. A. (1995) J. Biol. Chem. **270**, 5490–5494
18 Schwartz, J.-L., Lu, Y.-J., Söhnlein, P., Brousseau, R., Laprade, R., Masson, L. and Adang, M. J. (1997) FEBS Lett. **412**, 270–276
19 Masson, L., Lu, Y.-J., Mazza, A., Brousseau, R. and Adang, M. J. (1995) J. Biol. Chem. **270**, 20309–20315
20 Masson, L., Mazza, A., Brousseau, R. and Tabashnik, B. (1995) J. Biol. Chem. **270**, 11887–11896
21 Stenberg, E., Person, B., Roos, H. and Urbaniczky, C. (1991) J. Colloid Interface Sci. **143**, 513–526
22 Van Rie, J., Jansens, S., Höfte, H., Degheele, D. and Van Mellaert, H. (1990) Appl. Environ. Microbiol. **56**, 1378–1385
23 Ihara, H., Kuroda, E., Wadano, A. and Himeno, M. (1993) Biosci. Biotech. Biochem. **57**, 200–204
24 Liang, Y., Patel, S. S. and Dean, D. H. (1995) J. Biol. Chem. **270**, 24719–24724
25 Kalb, E. and Tamm, L. K. (1992) Biochim. Biophys. Acta **1103**, 307–316
26 Garczynski, S. F., Crim, J. W. and Adang, M. J. (1991) Appl. Environ. Microbiol. **57**, 2816–2820
27 Smedley, D. P. and Ellar, D. J. (1996) Microbiology **142**, 1617–1624
28 Stewart, G. S. A. B., Johnstone, K., Hagelberg, E. and Ellar, D. J. (1981) Biochem. J. **198**, 101–106
29 Bell, R. A. and Joachim, F. G. (1976) Ann. Entomol. Soc. Am. **69**, 365–373
30 Wolfersberger, M. G., Lüthy, P., Maurer, A., Parenti, P., Sacchi, V. F., Giordana, B. and Hanozet, G. M. (1987) Comp. Biochem. Physiol. **86A**, 301–308
31 Bradford, M. M. (1976) Anal. Biochem. **72**, 248–254
32 Carroll, J. and Ellar, D. J. (1997) Eur. J. Biochem. **245**, 797–804
33 Finney, D. J. (1952) Probit Analysis, 2nd edn., Cambridge University Press, Cambridge
34 Lieberman, H. R. (1983) Drug Chem. Toxicol. **6**, 111–116
35 Cooper, M. A., Williams, D. H. and Cho, Y. R. (1997) Chem. Commun. 1625–1626
36 Bietlot, H. P., Carey, P. R., Choma, C., Kaplan, H., Lessard, T. and Poszgay, M. (1989) Biochem. J. **260**, 87–91
37 Burden, R. L. and Faires, J. D. (1993) Numerical Analysis, 5th edn., PWS-Kent Publishing Company, Boston, MA
38 Myszka, D. G., Morton, T. A., Doyle, M. L. and Chaiken, I. M. (1997) Biophys. Chem. **64**, 127–137
39 Karlsson, R. and Falt, A. (1997) J. Immunol. Methods **200**, 121–133
40 Li, J., Carroll, J. and Ellar, D. J. (1991) Nature (London) **353**, 815–821
41 Grochulski, P., Masson, L., Borisova, S., Pusztai-Carey, M., Schwartz, J. L., Brousseau, R. and Cygler, M. (1995) J. Mol. Biol. **254**, 447–464
42 Dean, D. H., Rajamohan, F., Lee, M. K., Wu, S.-J., Chen, X. J., Alcantara, E. and Hussain, S. R. (1996) Gene **179**, 111–117
43 Wu, D. and Aronson, A. I. (1992) J. Biol. Chem. **267**, 2311–2317
44 Ahmad, W. and Ellar, D. J. (1990) FEMS Microbiol. Lett. **68**, 97–104
45 Chen, X. J., Curtiss, A., Alcantara, E. and Dean, D. H. (1995) J. Biol. Chem. **270**, 6412–6419
46 Garczynski, S. F. and Adang, M. J. (1995) Insect Biochem. Mol. Biol. **25**, 409–415
47 Knight, P. J. K., Knowles, B. H. and Ellar, D. J. (1995) J. Biol. Chem. **270**, 17765–17770
48 Knowles, B. H., Knight, P. J. K. and Ellar, D. J. (1991) Proc. R. Soc. London B **245**, 31–35

Received 13 October 1997/16 March 1998; accepted 6 May 1998